Electronic Supplementary Material (ESI) for Journal of Materials Chemistry C.

SUPPORTING INFORMATION

Triple-signaling mechanisms-based three-in-one multi channel chemosensor for discriminating Cu^{2+}, acetate and ion pair mimicking AND, NOR, INH and IMP logic functions

Prabhpreet Singh[a,*], Harminder Singh[a] , Gaurav Bhargava[b] and Subodh Kumar[a]

[a]*Department of Chemistry, UGC Centre for Advanced Studies, Guru Nanak Dev University, Amritsar 143 005, India. E-mail:prabhpreet.chem@gndu.ac.in; Tel: +91-84271-01534*

[b]*Department of Applied Sciences, Punjab Technical University, Kapurthala-144601, Punjab, India.*

Table of Contents

1. Experimental and synthesis of compounds

Chemicals and solvents were of reagent grade and used without further purification unless otherwise stated. All reactions were performed under N_2 atmosphere. Acetonitrile (HPLC grade) and ethanol were purchased from Spectrochem India Ltd and Changshu Yangyuan Chemical China respectively. Chromatographic purification was done with silica gel 60-120 mesh. TLC was performed on aluminium sheets coated with silica gel 60 F254 (Merck, Darmstadt). NMR spectra were recorded on Bruker and JEOL (operating at 500 and 300 for ^{1}H; 125 and 75 MHz for ^{13}C, respectively). The peak values were obtained as ppm (δ), and referenced to the TMS as reference in ^{1}H NMR and deutrated solvent in ^{13}C NMR spectra. Abbreviations used for splitting patterns are s = singlet, bs = broad singlet, t = triplet, q = quartet, m = multiplet. Fourier transform infrared (FT-IR) spectra were recorded on Perkin Elmer 92035. The fluorescence spectra were recorded by excitation at 330 nm unless otherwise stated. The fluorescence titrations were performed on Varian Carey Eclipse fluorescence and BH Chronos spectrophotometer. The absorption spectra were recorded on Shimadzu-2450 spectrophotometer from Shimadzu. HRMS spectra were recorded on Bruker MicroToff/QII. ^{1}H NMR titration of **1** against acetate (AcO^-) was performed in DMSO (d_6) on JEOL 300 MHz spectrometer. All the data were then processed in Top Spin software to draw the stacking spectra. Threotical calculations were carried out using density functional theory (DFT) at B3LYP/6-31G(d,p) basis set. The solutions of chemosensor **1-3** were prepared in acetonitrile (HPLC grade). The solutions of metal perchlorates and anions as tetrabutylammonium salt were prepared in acetonitrile (HPLC grade) and were added in microliter quantities. All absorption and fluorescence scans were saved as ACS II files and further processed in Excel™ to produce all graphs shown. The spectral data were analyzed through curve fitting procedures by using non-linear regression analysis SPECFIT 3.0.36 to determine the stability constants and the distribution of various species. The intermediate compounds **4,5**[1] and **6**[2] were synthesized after modification of the literature procedures.

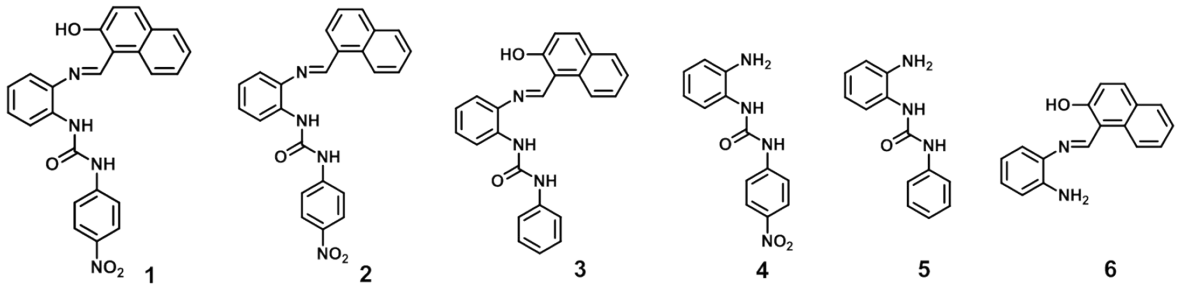

*MOLECULAR STRUCTURE OF COMPOUNDS **1-6***

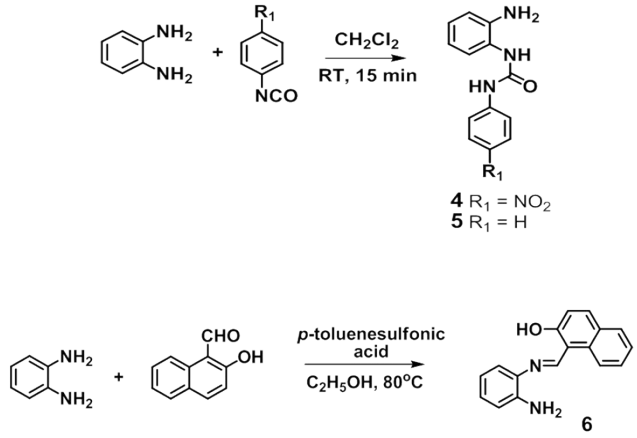

Scheme SI-1 Synthetic scheme for compounds **4-6**.

Synthesis of compounds 4 and 5

General procedure**:** To a solution of *o*-phenylenediamine (300 mg, 2.776 mmol) in dichloromethane, 4-nitrophenyl isocyanate (454 mg, 2.776 mmol) was added and reaction mixture was stirred vigorously at room temperature for about 1 hour (Scheme SI-1). The progress of the reaction was monitored by TLC. During this time interval, pale yellow precipitates separated in reaction mixture. After completion of reaction the product was isolated by suction filtration.

Compound 4: Yellow solid (570 mg, 76%). R_f = 0.50 (50% ethyl acetate:hexane); ^{1}H NMR (500 MHz, DMSO-d_6) δ 9.53 (s, 1H) , 8.19 (d, 2H, J = 10 Hz), 7.93 (s, 1H), 7.69 (d, 2H, J = 5 Hz), 7.32 (d, 1H, J = 10 Hz), 6.89 (t, 1H, J = 10 Hz), 6.76 (d, 1H, J = 10 Hz), 6.60 (t, 1H, J = 5 Hz), 4.85 (s, 2H) ppm; ^{13}C NMR (125 MHz, DMSO-d_6) δ 153.0, 147.2, 141.9, 141.2, 125.6, 125.6, 124.8, 124.2, 117.6, 117.2, 116.4 ppm; HRMS (TOF MS ESI) calculated for $C_{13}H_{12}N_4O_3$, *m/z* 272.0909; found 295.0779 ($M+Na^+$).

Compound 5: Pale yellow solid (500 mg, 96%). R_f = 0.60 (50% ethyl acetate:hexane); ^{1}H NMR (500 MHz, DMSO-d_6) δ 8.75 (s, 1H), 7.72 (s, 1H), 7.45 (d, 2H, J = 9 Hz), 7.34 (d, 1H, J = 8 Hz), 7.27 (t, 2H, J = 7.5 Hz), 6.95 (t, 1H, J = 8 Hz), 6.85 (t, 1H, J = 8.5 Hz), 6.75 (d, 1H, J = 7.5 Hz), 6.58 (t, 1H, J = 8Hz), 4.79 (s, 2H) ppm; ^{13}C NMR (125 MHz, DMSO-d_6) δ 153.6, 141.3, 140.5, 129.2, 135.2, 124.9, 124.2, 121.9, 118.4, 117.3, 116.4 ppm; HRMS (TOF MS ESI) calculated for $C_{13}H_{13}N_3O$, *m/z* 227.0909; found 228.1039 ($M+H^+$).

Synthesis of compound 6

The stirring of 1:1 mixture of 2-hydroxy-1-naphthaldehyde (800 mg, 4.6236 mmol) and *o*-phenylenediamine (500 mg, 4.6236 mmol) in chloroform and ethanol (1:9 v/v) with catalytic amount of *p*-toluenesulfonic acid were carried out for 2h at 80°C. The progress of the reaction was monitored with the help of TLC. During this time interval, yellow solid precipitated out in the reaction mixture. The yellow solid was filtered out and washed with ethanol to isolate pure compound **6**, Yield 79 %; R_f = 0.30 (20% ethyl acetate: hexane); ^{1}H NMR (500 MHz, $CDCl_3$) δ 15.22 (s, 1H) , 9.43 (s, 1H), 8.16 (d, 1H, *J* = 8 Hz), 7.83 (d, 1H, *J* = 9 Hz), 7.76 (d, 1H, *J* = 8 Hz), 7.53 (t, 1H, *J* = 7.0 Hz), 7.36 (t, 1H, *J* = 8 Hz), 7.18-7.15 (m, 2H), 7.12 (t, 1H, *J* = 8 Hz), 6.86 - 6.80 (m, 2H), 4.00 (s, 2H).

2. Solvent effect and their photophysical and spectroscopic properties

Table S1: Spectroscopic characteristics of chemosensors **1-3** in CH_3CN.

Chemosensor	λ_{abs} (nm)	λ_{em} (nm)	ν_{abs}[a] x10^4 (cm^{-1})	ν_{flu}[b] x10^4 (cm^{-1})	$(\nu_A - \nu_F)$[c] (cm^{-1})
1	337	458	2.967	2.183	7840
2	327	411	3.058	2.433	6250
3	380	456	2.631	2.192	4390

[a]maximum absorption wavenumbers. [b]maximum fluorescent wavenumbers. [c]Stoke's shift.

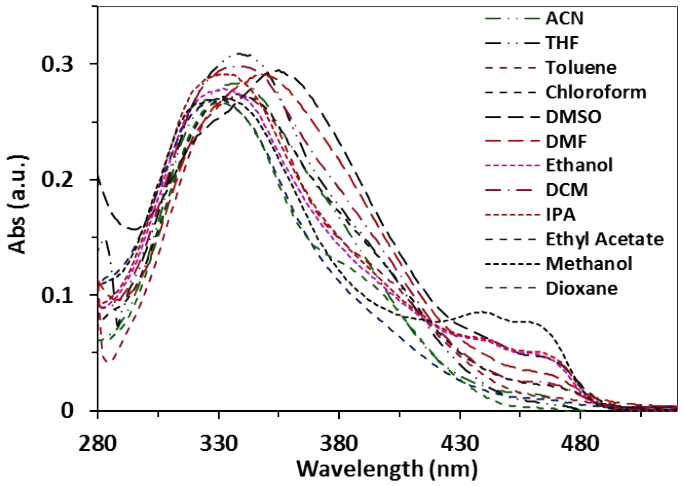

Fig. S1a Effect of solvent polarity on the UV-Vis absorption intensity of chemosensor **1**, showing solvatochromism phenomena.

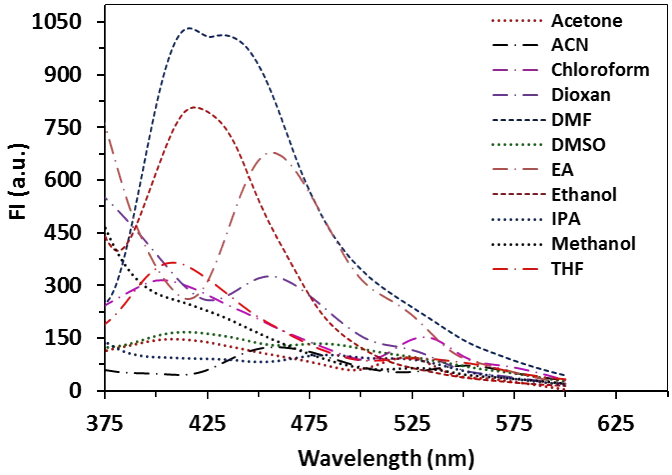

Fig. S1b Effect of solvent polarity on the fluorescence intensity of chemosensor **1**, showing solvatofluorism phenomena.

Table S2: Spectroscopic characteristics of chemosensors **1** in different solvents.

Solvent	**λ_{Abs} (nm)**	**λ_{em} (nm)**	**ν_{abs}[a] x10^4 (cm^{-1})**	**ν_{flu}[b] x10^4 (cm^{-1})**	**Δf[c]**	**($\nu_A - \nu_F$)[d] (cm^{-1})**
Dioxane	330	455	3.030	2.197	0.0294	8330
Toluene	340	456	2.941	2.192		7490
Chloroform	334	400	2.994	2.500	0.1491	4940
Ethyl acetate	327	455	3.058	2.197		8610
Tetrahydrofuran	338	408	2.958	2.450		5080
Dichloromethane	334	477	2.994	2.096		8980
IPA	330	418	3.030	2.392	0.2769	6380
Ethanol	332	419	3.012	2.386	0.2887	6260
Methanol	329	413	3.039	2.421	0.3093	6180
CH_3CN	337	458	2.967	2.183	0.3054	7840
DMF	349	416	2.865	2.403	0.2750	4620
DMSO	355	414	2.816	2.415	0.2637	4010

[a]maximum absorption wavenumbers. [b]maximum fluorescent wavenumbers. [c]Lippert-Mataga polarity parameter (Δf) [29]. [d]Stoke's shift.

3. Jobs Plot

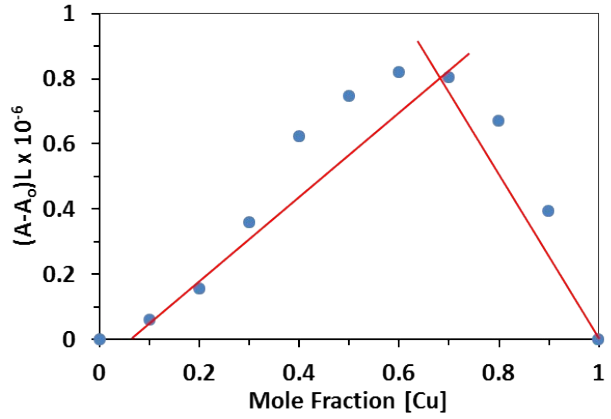

Fig. S2 Job's plot showing **1**:Cu^{2+} (1:2) complex recorded in CH_3CN solution.

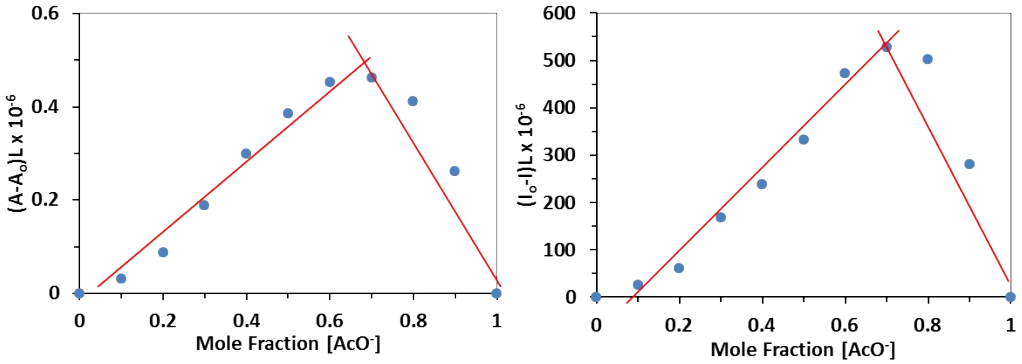

Fig. S5 Job's plot (Colorimetrically and fluorometrically) showing **1**:AcO^- (1:2) complex recorded in CH_3CN solution.

4. Photophysical behaviour of chemosensor 2 and 3 with Cu^{2+} ion

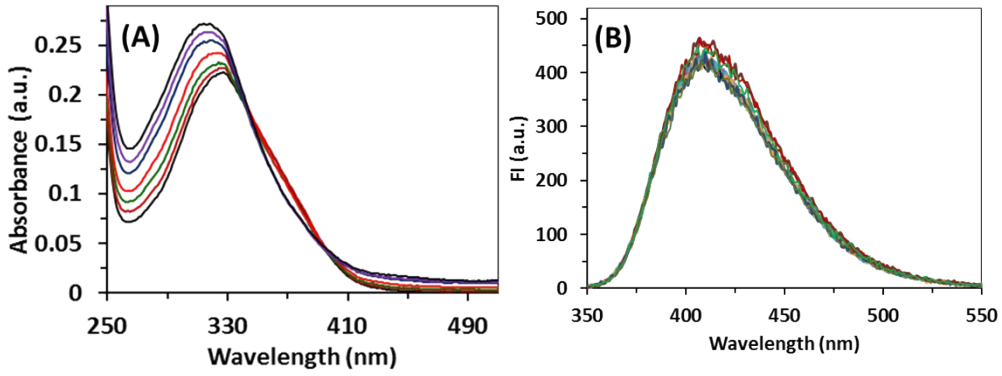

Fig. S3 (A) UV-Vis spectra (B) Fluorescence emission spectra of **2** (10 μM) on addition of Cu^{2+} ions. λ_{ex} 330 nm. Slit width (Ex/Em = 5 nm).

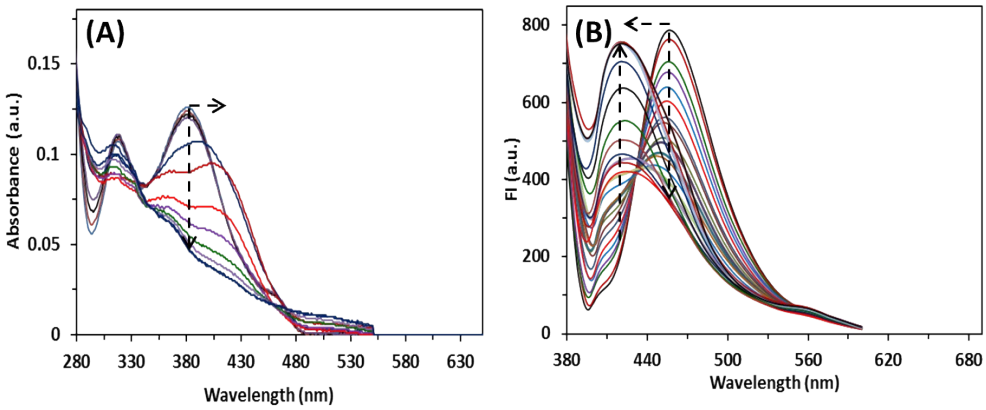

Fig. S4 (A) UV-Vis spectra of **3** (10 μM) on addition of Cu^{2+} ions; (B) Fluorescence spectra of **3** (10 μM) on addition of Cu^{2+} ions. λ_{ex} 370 nm. Slit width (Ex/Em = 10 nm).

5. Photophysical behaviour of chemosensor 2 and 3 with Acetate ion

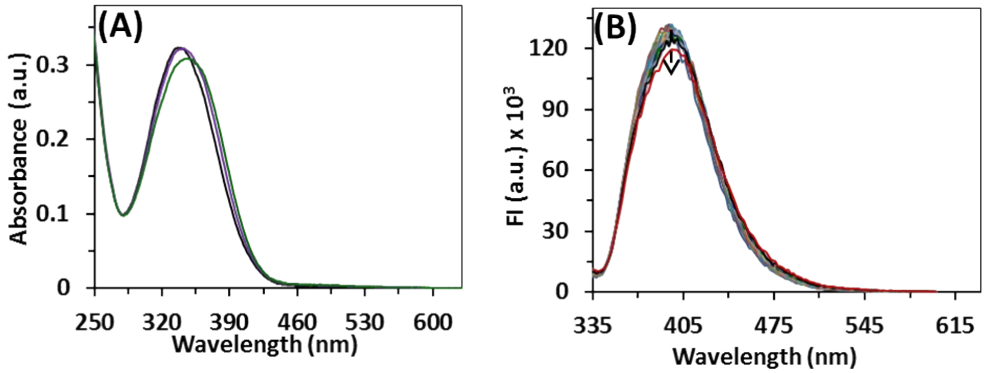

Fig. S6 (A) UV-Vis spectra of chemosensor **2** (10 μM) on addition of the acetate ions; (B) Fluorescence emission spectra of chemosensor **2** (10 μM) on addition of the acetate ions. λ_{ex} 370 nm. Slit width (Ex/Em = 10 nm).

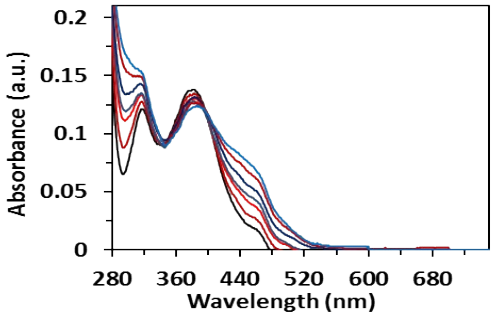

Fig. S7 (A) UV-Vis spectra of chemosensor **3** (10 μM) on addition of acetate ions.

6. Photophysical behaviour of chemosensor 1 with Ion pairs

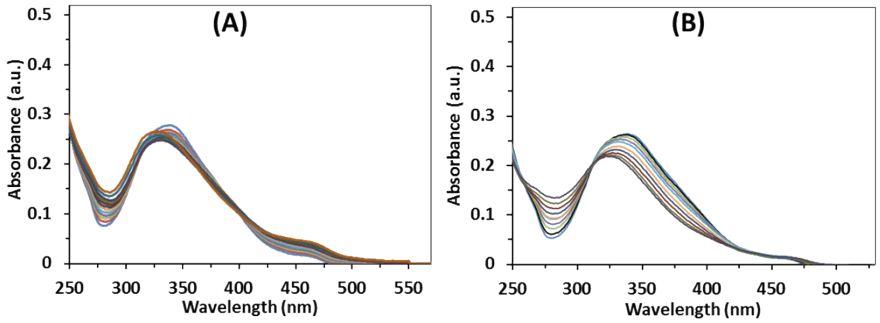

Fig. S8 UV-Vis spectra of chemosensor **1** (10 µM) on addition of (A) $CuCl_2$ solution and (B) $Cu(NO_3)_2$ solution.

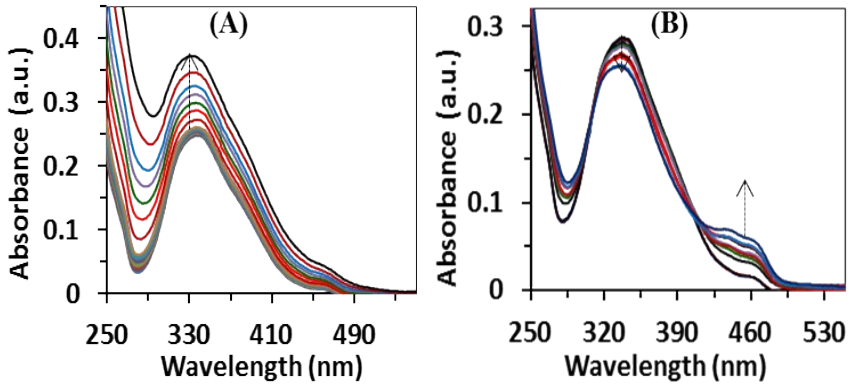

Fig. S9 UV-Vis spectra of chemosensor **1** (10 µM) on addition of (A) $Pd(OAc)_2$ solution and (B) $Hg(OAc)_2$ solution.

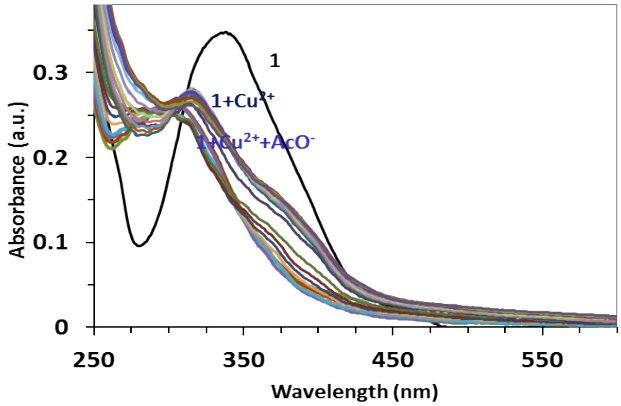

Fig. S10 UV-Vis spectra of (**1**+Cu^{2+}) complex (10 µM of **1** and 50 µM of Cu^{2+}) on gradual addition of the acetate solution.

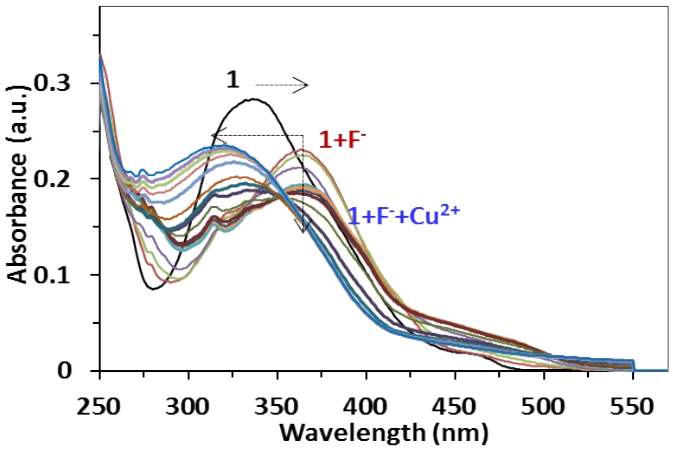

Fig. S11 UV-Vis spectra of (**1**+F^-) complex (10 µM of **1** and 50 µM of F^-) on gradual addition of the copper ion solution.

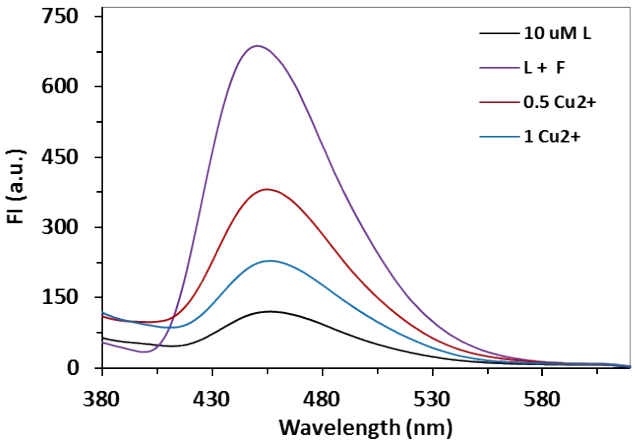

Fig. S12 Fluorescence spectra of (**1**+F^-) complex (10 µM of **1** and 50 µM of F^-) on gradual addition of the copper ion solution.

7. Photophysical behaviour of chemosensor 2 and 3 with $Cu(AcO)_2$ Ion pair

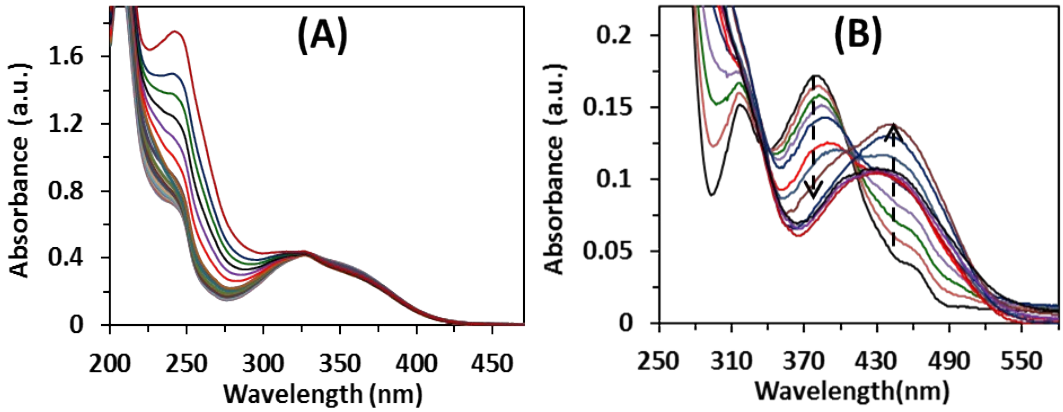

Fig. S13 (A) UV-Vis spectra of **2** (10 μM) and (B) UV-Vis spectra of **3** (10 μM) on addition of the $Cu(OAc)_2$ solution.

8. Interference studies for $Cu(OAc)_2$ ion pair

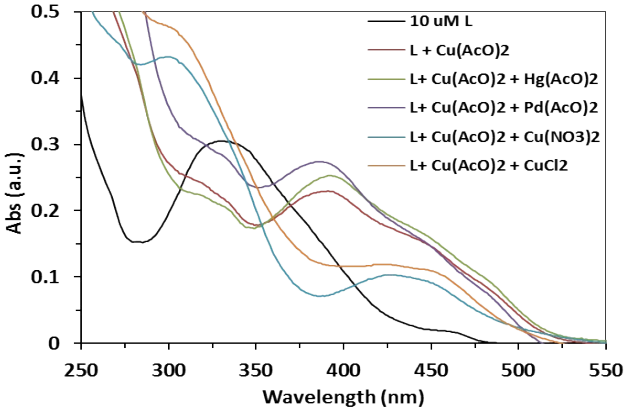

Fig. S14 Effect of different ion pairs on the absorbance intensity of **1** (10 μM) by copper acetate alone (100 μM) and other competitive ion pairs (300 μM).

9. ^{1}H NMR titration studies

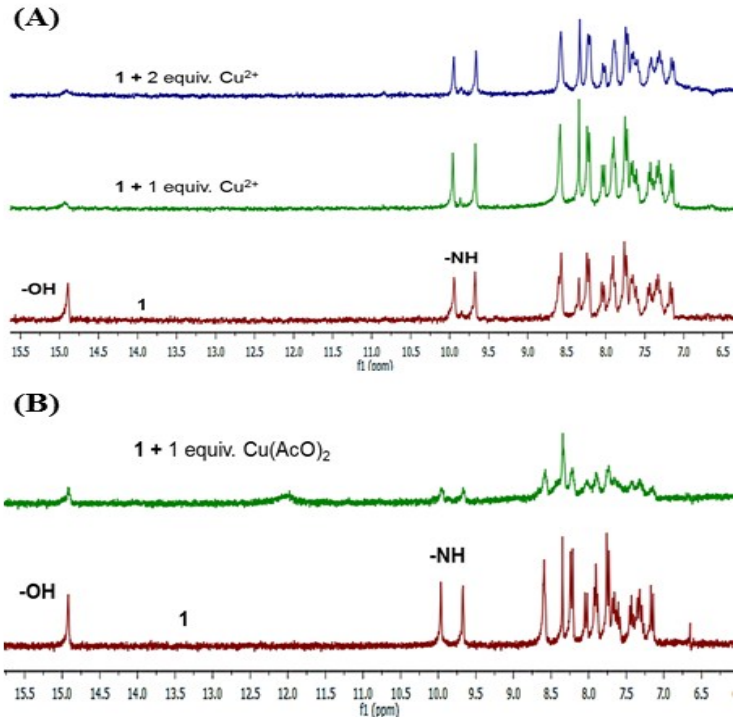

Fig. S15 Partial ^{1}H NMR spectrum of chromo-fluorescent sensor **1** recorded in DMSO-d_6 at different addition (in equivalent) of (A) $Cu(ClO_4)_2$ and (B) $Cu(OAc)_2$.

10. Photophysical properties of compounds 4 and 6 (as controls)

The control compounds **4** and **5** showed non-emissive behaviour in the fluorescence, when excited at 330 nm. The absorption spectrum of **4** on addition of Cu^{2+} ions shows blue shift from 337 to 303 nm (~34 nm) up to addition of 50 μM of Cu^{2+} ions Similarly, the absorption spectrum of **4** on addition of acetate ions shows red shift from 337 to 360 nm (~23 nm) up to addition of 100 μM of acetate ions and then attained the plateau.

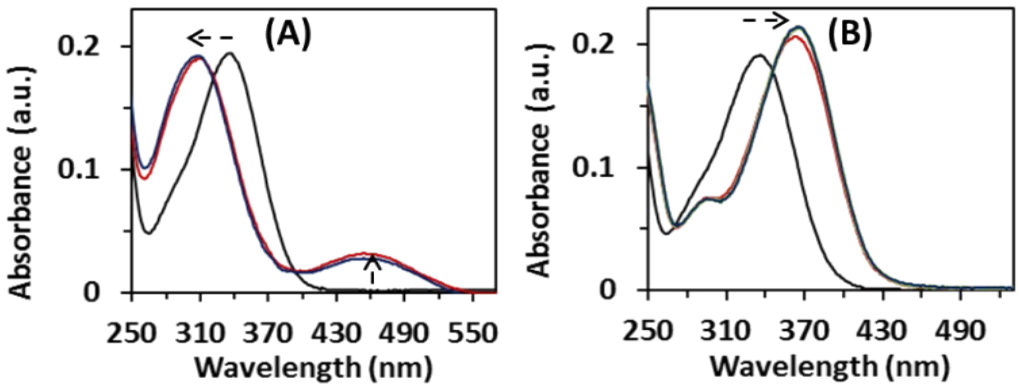

Fig. S16 UV-Vis spectra of **4** (10 μM) on addition of the (A) Cu^{2+} and (B) acetate ions.

The absorption spectrum of **6** on addition of Cu^{2+} up to 500 μM shows decrease in intensity at 397 nm. When excited at 330 nm, fluorescence emission maxima of **6** at 458 nm was quenched on addition of low concentration of Cu^{2+} followed by large enhancement of fluorescence intensity with concomitant blue-shift of emission maxima to 427 nm at high concentration of Cu^{2+} ions.

The UV-Vis titration of **6** in CH_3CN with acetate ions shows no change in the absorption spectra. However, the fluorescence titration of **6** in CH_3CN against AcO^- ions showed ~4 time increase in fluorescence intensity at 458 nm.

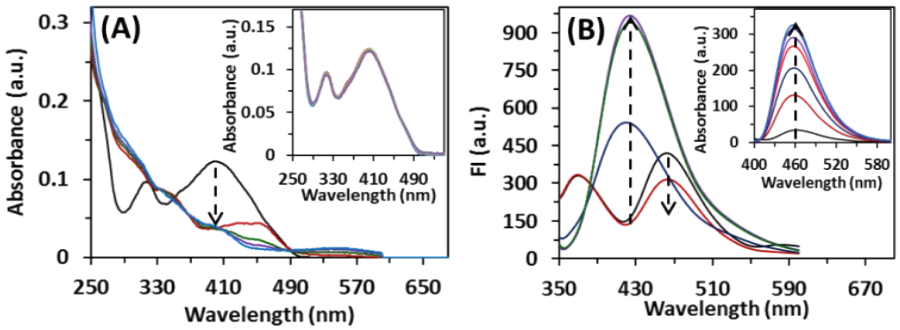

Fig. S17 (A) UV-Vis spectra of **6** (10 μM) on addition of the Cu^{2+} ions. Inset: UV-Vis spectra of **6** (10 μM) on addition of the AcO^- ions. (B) Fluorescence spectra of **6** (10 μM) on addition of the Cu^{2+} ions; λ_{ex} 370 nm. Slit width (Ex = 10 nm, Em = 10 nm). Inset: Fluorescence spectra of **6** (10 μM) on addition of the AcO^- ions; λ_{ex} 370 nm. Slit width (Ex = 10 nm, Em = 10 nm).

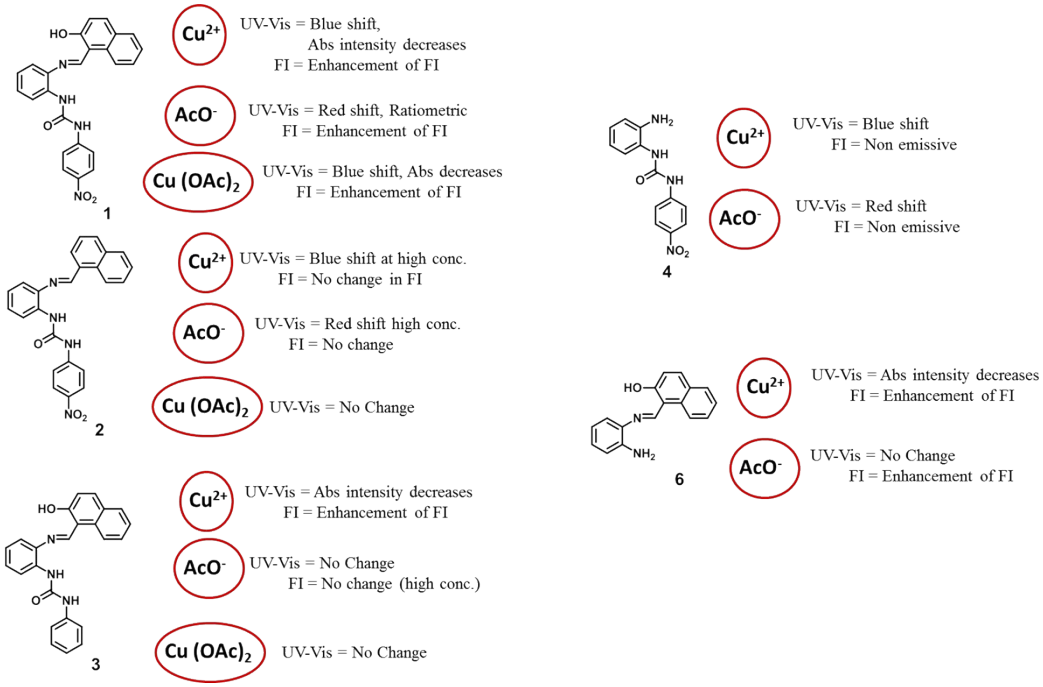

Interaction of Cu^{2+} ions

Absorbance: Comparing **1** with **4** and **6**, it is clear that chemosensor **1** utilizes both binding sites for complexation with Cu^{2+}, AcO^- and $Cu(AcO)_2$ ion pair. On the other hand, chemosensor **2** deprived of –OH, lost complexation with Cu^{2+}, whereas chemosensor **3** shows decreased acidity due to absence of $–NO_2$ group and lost the affinity for complexation with Cu^{2+} ions at the urea binding site. The participation of urea moiety in complexation with Cu^{2+} is also evident from blue-shift of nitroaniline absorption maxima from 337 nm to 308 nm, on addition of Cu^{2+} to the solution of chemosensor **1**.

Emission: Comparing **1** with **4** and **6**, it seems that Schiff base moiety is responsible for the observed changes in their fluorescence spectrum. On the other hand chemosensor **2** deprived of –OH shows no fluorescence change whereas chemosensor **3** show similar behaviors in fluorescence titration on addition of Cu^{2+} ions as observed for chemosensor **1**.

Interaction of Acetate Ions

Absorbance: Comparing **1**, **2** and **4**, it seems that addition of AcO^- ions results in red shift of the absorption band with exception of ratiometric behavior in UV-Vis spectrum i.e. A_{354nm}/A_{326nm} only in case of **1** and **4**. Chemosensor **2** requires high concentration of acetate ions to undergo red shift.

Emission: **4** show non-emissive behavior in fluorescence spectrum, when excited at 330 nm. This fact was further confirmed when titration of AcO^- with chemosensor **3** and control compound **6** shows similar fluorescence enhancement at 458 nm. Therefore, AcO^- also interact at both urea and Schiff base moieties of **1** to cause red-shift in absorption band from 337 to 360 nm and increase in fluorescence intensity of the Schiff base moiety at 458 nm.

Interaction with Copper acetate ion pair

As expected only Chemosensor **1** shows dual channel monitoring with $Cu(AcO)_2$ ion pair due to presence of binding sites for each ion pair, whereas no change was observed with chemosensor **2** and **3** which lacks one of the two binding sites.

11. Interference experiments for chemosensor 1 for Cu^{2+} and acetate ion recognition

The absorption spectrum of **1** on addition of Cu^{2+} (50 μM) shows blue shift from 337 to 308 nm. On addition of 150 μM of various cations such as Ni^{2+}, Pb^{2+}, Co^{2+}, Ba^{2+}, Sr^{2+}, Na^{+} and 50 μM of Hg^{2+}, Zn^{2+} did not cause any further spectral change in the absorption spectrum. The spectral changes (red shift in the absorption spectrum and 'turn on' behaviour in fluorescence spectrum) obtained after addition of acetate were retained even on addition of 300 μM of various anions such as $H_2PO_4^-$, ClO_4^-, HSO_4^-, I^-, Br^- and 100 μM of F^- and CN^- ions.

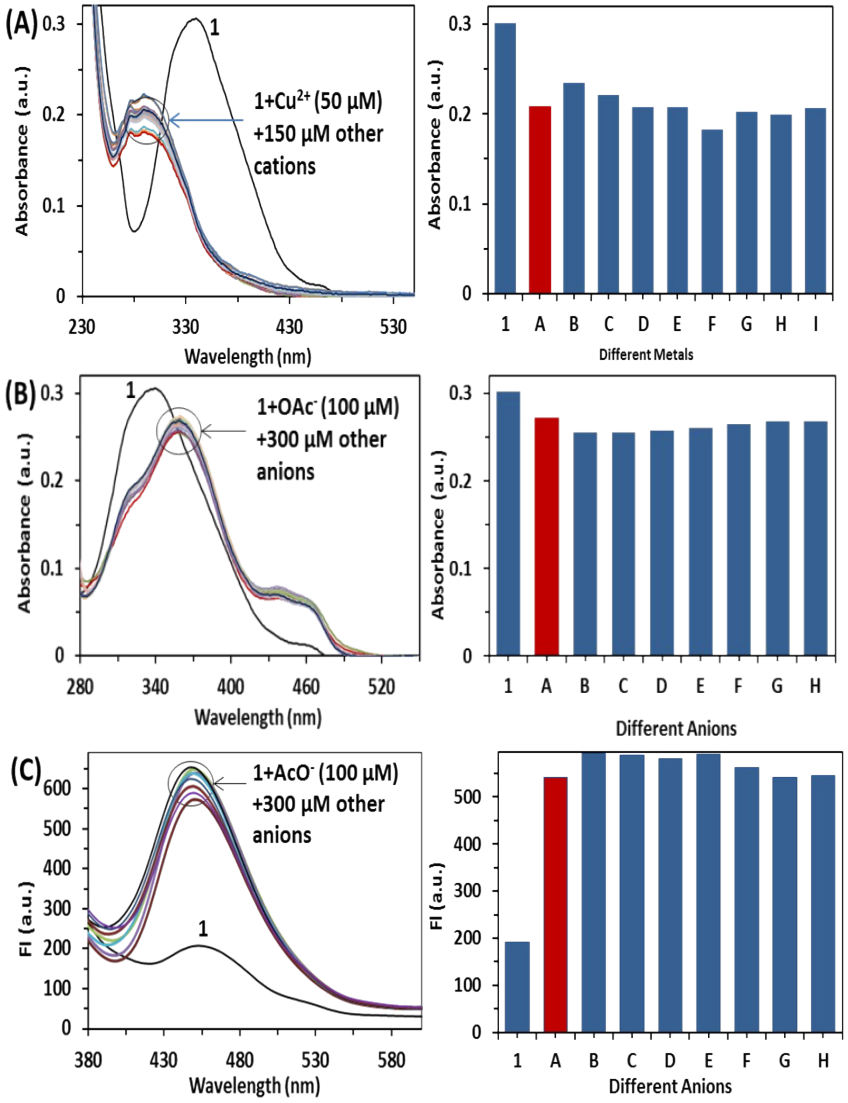

Fig. S18 (A) Absorbance spectra of chemosensor **1** (10 μM) in response to Cu^{2+} (50 μM) in the presence of various metal ions (150 μM); Bar graph where red bar represent absorption λ_{abs} = 308 nm of chemosensor **1** (10 μM) upon addition of A = Cu^{2+} (50 μM) ions; Blue bars, B = Hg^{2+} (50 μM), C = Ni^{2+}; D = Pb^{2+}, E = Co^{2+}, F = Zn^{2+} (50 μM); G = Ba^{2+}; H = Sr^{2+}; I = Na^{+} (150 μM); (B) Absorbance and (C) Fluorescence spectra of chemosensor **1** (10 μM) in response to AcO^- (50 μM) in the presence of various anions (300 μM); Bar graph where red bar represent absorption (λ_{abs} = 360 nm) and emission (λ_{em} = 458 nm) of chemosensor **1** (10 μM,) upon addition of A = acetate (100 μM) ions; Blue bars B = F^-; C = CN^- (100 μM),; D = $H_2PO_4^-$; E = ClO_4^-; F = HSO_4^-; G = I^-; H = Br^-. In all bar graphs blue bar **1** is chemosensor **1** with λ_{abs} = 337 nm and λ_{em} = 458 nm).

References

1. W. Jiamin, L. Shaoguang, Y. Peiju, H. Xiaojuan, J.Y. Xiao and W. Biao, *CrystEngComm.*, 2013, ***15****, 4540.*
2. M. Sahin, N. Kocak, D. Erdenay and U. Arslan, *Spectrochimica Acta, Part A: Mol. Biomol. Spect.*, 2013, **103**, 400.